Title

Neurotoxicity of the Parkinson Disease-Associated Pesticide Ziram Is Synuclein-Dependent in Zebrafish Embryos

Authors

Lulla, Aaron

Barnhill, Lisa

Bitan, Gal

et al.

Peer reviewed

Neurotoxicity of the Parkinson's Disease-Associated Pesticide Ziram Is Synuclein-Dependent in Zebrafish Embryos

Aaron Lulla, Lisa Barnhill, Gal Bitan, Magdalena I. Ivanova, Binh Nguyen, Kelley O'Donnell, Mark C. Stahl, Chase Yamashiro, Frank-Gerrit Klärner, Thomas Schrader, Alvaro Sagasti, and Jeff M. Bronstein

Neurotoxicity of the Parkinson's Disease-Associated Pesticide Ziram Is Synuclein-Dependent in Zebrafish Embryos

Aaron Lulla[1], Lisa Barnhill[1], Gal Bitan[1,5,6], Magdalena I. Ivanova[2,7], Binh Nguyen[1], Kelley O'Donnell[3] ,Mark C. Stahl[1], Chase Yamashiro[1], Frank-Gerrit Klärner[8], Thomas Schrader[8], Alvaro Sagasti[3], and Jeff M. Bronstein[1,4,5]

[1]Departments of Neurology, [2]Chemistry and Biochemistry, [3]Molecular, Cell, and Developmental Biology, UCLA, Los Angeles, California, USA; [4]Parkinson's Disease Research, Education, and Clinical Center, Greater Los Angeles Veterans Affairs Medical Center, Los Angeles, California, USA; [5]Brain Research Institute, [6]Molecular Biology Institute, and [7]UCLA-DOE Institute, UCLA, Los Angeles, California; [8]Institute of Organic Chemistry, University of Duisburg-Essen, Essen 45117, Germany.

Address correspondence to Jeff M. Bronstein, David Geffen School of Medicine at UCLA, Department of Neurology, 710 Westwood Plaza, Los Angeles, CA 90095-1769 USA. Telephone: 310 206-9799. E-mail: jbronste@mednet.ucla.edu.

Magdalena I. Ivanova's present address: Department of Neurology and Program of Biophysics, University of Michigan, Ann Arbor, MI 48109. Mark C Stahl's present address: Department of Neurology, Pennsylvania State University Milton S. Hershey Medical Center, Hershey, PA 17033.

Running title: Neurotoxicity of Ziram is Synuclein Dependent

Conflict of Interests: GB, F-GK, and TS are co-inventors of US patent No. 8,791,092 and

European Patent Application 10 708 075.6, Molecular Tweezers for the Treatment of Amyloid-

Related Diseases. The other authors declare they have no actual or potential competing financial

interests.

Abstract

Exposure to the commonly used dithiocarbamate (DTC) pesticide ziram is associated with an increased risk of developing Parkinson's disease (PD), although the mechanisms of toxicity are not completely understood. In this study, we utilized zebrafish (ZF) embryos to study the mechanisms of ziram's neurotoxicity *in vivo*. Nanomolar concentrations of ziram caused selective loss of dopaminergic (DA) neurons and impaired swimming behavior. Since ziram increases α-synuclein (α-syn) concentrations in rat primary neuronal cultures, we investigated the effect of ziram on ZF γ-synuclein 1 (γ1). ZF express 3 synuclein isoforms and ZF γ1 appears to be a functional homologue of α-syn. We found that recombinant ZF γ1 formed fibrils *in vitro* and overexpression of ZF γ1 in ZF embryos led to the formation of neuronal aggregates and neurotoxicity similarly to α-syn. Importantly, knockdown of ZF γ1 with morpholinos or disruption of oligomers with the molecular tweezer CLR01 prevented ziram's DA toxicity. These data demonstrate that ziram is selectively toxic to DA neurons *in vivo* and this toxicity is synuclein-dependent. These findings have important implications for understanding the mechanisms by which pesticides may cause PD.

Introduction

Parkinson's disease (PD) is a neurodegenerative disease that affects millions of individuals worldwide (Dorsey et al. 2007). Although significant progress has been made in understanding the pathophysiology of PD, the etiology is still not well understood. There does not appear to be one simple cause of PD but it likely develops from complex genetic and environmental interactions.

Several lines of evidence have implicated the involvement of α-synuclein (α-syn) in the pathogenesis of PD. The identification of mutations in the α-syn- (SNCA) gene led to the finding that α-syn is the major component of Lewy Bodies the pathological hallmark of PD, not only in these patients, but also in sporadic PD (Baba et al. 1998; Chartier-Harlin et al. 2004; Farrer et al. 2004; Ibanez et al. 2004; Kruger et al. 1998; Nishioka et al. 2006; Polymeropoulos et al. 1997; Singleton et al. 2003; Spillantini et al. 1997). Additionally, overexpression of wild-type (WT) α-syn by gene multiplication causes fairly typical PD (Hope et al. 2004). Furthermore, people who carry an allele in the α-syn promoter (REP1 263) that confers a higher level of expression are at higher risk of developing PD (Maraganore et al. 2006). Thus, increased expression of α-syn increases the risk of developing PD and if expression is doubled or more, one will get the disease. REP1 263 is also associated with faster progression of PD adding further support for the concept that increased levels of α-syn is central to the pathogenesis of PD (Ritz et al. 2012). More recently, evidence is building that α-syn expression may also interact with environmental factors to increase the risk of developing the disease. For example, the REP1 263 allele, influences susceptibility to damage from paraquat exposure and head trauma (Gatto et al. 2010; Goldman et al. 2012).

The genetics of PD have been extensively studied but only account for a small percentage of patients with PD, suggesting that environmental factors play an important role (International Parkinson Disease Genomics et al. 2011; Trinh and Farrer 2013). Epidemiological studies have demonstrated that pesticide exposure is associated with an increased risk of developing PD (Brown et al. 2006; Goldman 2014) and a causal role for this association is supported by cell-based and animal studies (Betarbet et al. 2000; Chou et al. 2008; Fitzmaurice et al. 2013; McCormack et al. 2002; Ryan et al. 2013; Thiruchelvam et al. 2000; Wang et al. 2006). Interestingly, the mechanisms by which pesticides increase disease risk appear to be diverse. Proposed mechanisms include mitochondrial inhibition, oxidative stress, impaired protein degradation, and aldehyde dehydrogenase (ALDH) inhibition (Barnhill and Bronstein 2014; Goldman 2014).

One pesticide of particular interest is the dithiocarbamate (DTC) fungicide ziram. Residential and workplace exposure to ziram is associated with a three fold increased risk for developing PD and as high as six fold for early onset cases (Wang et al. 2011). Additionally *in vitro* and *in vivo* exposure studies have shown that ziram is toxic to dopaminergic (DA) neurons in rat primary neuronal cultures (Chou et al. 2008). The mechanism of ziram's DA toxicity appears to be, at least in part, related to its ability to impair protein degradation by inhibiting E1 ligase of the ubiquitin proteasome system (UPS) and causing accumulation of α-syn (Chou et al. 2008).

Despite the progress that has been made in understanding the mechanisms of ziram's toxicity, *in vivo* studies are lacking. One reason for this is that testing in rodent models is very expensive and time consuming. Zebrafish (*Danio rerio*, ZF) are a powerful model organism to study the effects of environmental toxins and neurodegenerative diseases since they are rapidly

developing vertebrates with a well- formed DA neuronal network similar to that of mammals

(Bretaud et al. 2007; Milanese et al. 2012; Schweitzer et al. 2012; Sheng et al. 2010; Wen et al.

2008; Xi et al. 2011), have many orthologues to human drug targets (Gunnarsson et al. 2008),

and alterations in homeostasis of proteins associated with PD have been found to cause similar

effects in ZF and other model organisms (Betarbet et al. 2000; Feany and Bender 2000;

Prabhudesai et al. 2012). Here, we utilized ZF to further study the neurotoxicity of ziram *in vivo*

and found that exposure to low concentrations led to damaged DA neurons and abnormal motor

behavior. ZF do not have an orthologue to human α-syn but ZF γ-synuclein 1 (γ1) appears to be

functionally similar to α-syn (Milanese et al. 2012). ZF γ1 was found to form fibrils when

overexpressed like human α-syn. Importantly, ziram's toxicity was found to be ZF γ1-

dependent.

Materials and Methods

Zebrafish

ZF lines (AB unless other wised stated) were bred and maintained at 28 °C in

recirculating water tanks on a regulated 14h light/10h dark cycle and fed twice a day with brine

shrimp. All experiments were carried out in accordance with UCLA Animal Research

Committee protocols. ZF expressing GFP driven by the vesicular monoamine transporter

promoter (VMAT2:GFP) were purchased from the UCLA core facility and used in this study to

identify VMAT2 (dopaminergic, (nor)adrenergic, serotonergic) neurons in whole embryos (Wen

et al. 2008). Peripheral sensory neurons (trigeminal and Rohon-Beard) were visualized using the

Tg(isl1[ss]:Gal4-VP16,UAS:EGFP)[zf154] transgenic line, which has been referred to as

Tg(sensory:GFP), and were obtained from Dr. Sagasti (Sagasti et al. 2005).

A ZF γ1-synuclein expression construct (γ1-DsRed) composed of a T2A bicistronic configuration, driven by the *HuC* neuronal promoter and expressing monomeric DsRed, was used as previously described (Prabhudesai et al. 2012). The T2A sequence is cleaved after translation generating two proteins from a single open reading frame and resulting in stoichiometric expression of the gene of interest and the fluorescent reporter (Tang et al. 2009). ZF embryos were injected with *HuC*-ZFγ1-T2A-DsRed or *HuC*-DsRed (control) cDNA (50ng/μL) at the single cell stage.

Morpholinos (Gene Tools LLC, Philomath OR) were injected (0.1mM) at the single-cell stage for ZF γ1 (CATTAGAACATCCATCCTGGACGCT, translational blocking) or non-targeting/scrambled (CCTCTTACCTCAGTTACAATTTATA), as previously described (see Fig. S1) (Milanese et al. 2012). The molecular tweezers CLR01 and CLR03 were prepared and purified as sodium salts, as described previously (Fokkens et al. 2005; Talbiersky et al. 2008). Specificity of the ZF γ1 morpholino (MO) was validated by SDS PAGE (see Fig. S1d).

Zebrafish Treatments

ZF embryos, 25-35 per treatment in 10 mL of E3 media (15mM NaCl, 0.5mM KCl, 1.0mM $MgSO_4$, 0.15mM KH_2PO_4, 0.05mM Na_2HPO_4, 1.0mM $CaCl_2$, 0.7mM $NaHCO_3$), were reared at 32 °C and exposed to varying concentrations of ziram (98.5% purity, Chem Service, West Chester PA). Embryos were exposed to 1 nM-1 μM (0.01%DMSO) ziram in E3 media at 5 hours post-fertilization (hpf) or 24 hpf in a 6-well plate for 5 days for confocal microscopy and 7 days post fertilization (dpf) for behavior. The concentrations of ziram used for the study were well below those used for spraying (approximately 8 mM) (Agency 2015) and necessary for fungicidal activity (30 uM) (Briquet et al. 1976). VMAT2:GFP embryos were co-treated with

10μM CLR01 (Fokkens et al. 2005; Prabhudesai et al. 2012; Sinha et al. 2011) and 50nM ziram.

Log-Rank test was used for statistical analysis.

Confocal Microscopy

VMAT2:GFP embryos (3 dpf and 5 dpf) were anesthetized using Tricane-S (Western

Chemicals Inc., Ferndale WA) at a final concentration 50 μg/mL, fixed in 4% paraformaldehyde

(PFA) overnight and mounted in 2% low-melting agarose. Embryos were imaged at 20X using a

Zeiss LSM 510 microscope. Approximately 100 1.1 μm optical sections were obtained for each

embryo. Section images were stacked and reconstituted into 2D and 3D images using ImageJ

(National Institutes of Health). Neuron count analyses were conducted in a blinded manner as

previously described (Fitzmaurice et al. 2013). For MO and CLR01 studies, neuron counts for

treatment groups were normalized to injection and treatment controls to account for variances in

fish clutches between days and for treatment and injection survival. Student's t-test was used for

statistical analysis

Histology

ZF embryos were dechorinated at 2 dpf, fixed in 4% PFA for 24 hours, immersed in 30%

sucrose overnight and cryosectioned (10-μm). For thioflavin S (ThS) staining, sections were

immersed in 0.5% ThS dissolved in PBS (Sigma-Aldrich, St. Louis MO), washed with ethanol

(80%), and then mounted with Vectashield+Dapi (Vector Laboratories, Burlingame CA).

Polyclonal antibodies specific for ZF γ1 were raised using a C-terminal peptide

CDFSHGGMEGGEGGE (Genscript, Piscataway NJ). These antibodies bound specifically to ZF

γ1 at the predicted mass (17 kDa) in ZF embryos and to recombinant γ1 (see Fig. S1a).

Furthermore, the ZF γ1 band in Western blots was markedly reduced in ZF after pre-absorption

with the ZF γ1 peptide used to raise the antibody (see Fig. S1c). Anti-ZF γ1 antibodies did not

recognize any rodent brain proteins (see Fig. S1a).

For immunohistochemistry, sections were blocked in 10% normal goat serum (Jackson

Labs, Bar Harbor ME), incubated with anti-ZF γ1 antibody (1:1000) followed by incubation with

an anti-rabbit-Alexa-Fluor 568 antibody (1:500, Life Technologies, Grand Island NY). The

sections were then mounted with Vectashield+Dapi.

Behavioral Analysis

ZF embryos (7 dpf) were placed in 10mL of E3 media and kept in the dark to avoid

degradation of added chemicals. Drug or vehicle (5 μM apomorphine, 25 μM haloperidol or

0.1% DMSO) were added and incubated for 30-minutes at 28°C prior to behavioral analysis.

Twelve fish from each treatment group were transferred to a square 96-well plate and maintained

in the dark for 10 minutes prior to behavioral analysis, which consisted of 10-minute alternating

cycles of light (100% light as specified by Zebralab, View Point, France) and dark (total 30

minutes in light and 30 minutes in dark). Movements greater than 2 millimeters were collected

every two minutes using the Zebralab system and analyzed for distance traveled. Embryos with

notochord malformations were excluded for behavioral analysis. Data were normalized to

vehicle controls to account for variances between fish clutches from different days. One-way

ANOVA was used for statistical analysis.

Western and Native Blots

ZF embryos (5 dpf) were anesthetized as described above, pooled (35 embryos per

treatment), de-yolked, lysed, and sonicated in either 1X-SDS buffer or 1X-Native PAGE sample

buffer (Life Technologies). Protein concentrations were determined using the BCA protein assay

(Thermo-Fisher, Rockford IL). Protein (75μg/lane) was loaded onto SDS-PAGE or Native-

PAGE gels and transferred using the XCell-II blotting system (Life Technologies). Membranes

were probed with ZF γ1 1° antibody (1:2500 dilution), or TH 1° antibody (1:2500, MAB 318:

Millipore) followed by donkey anti-rabbit HRP 2° antibody (1:2500 dilution, Santa Cruz

Biotechnology, Dallas TX). Chemiluminescent substrate (Super Signal West Dura, Thermo

Scientific) was used for band visualization. α-Tubulin (1:500, Sigma-Aldrich) was used as a

loading control. Student's t-test was used for statistical analysis.

Expression and purification of zebrafish synuclein

Competent BL21 (DE3) E. Coli bacteria were transformed with a plasmid containing

the ZF synuclein gene, allowed to grow in 3 L Luria broth to $OD_{600} \approx 0.8$, induced with 0.5 mM

isopropyl β-D-1-thiogalactopyranoside and incubated for 3 additional hours. The bacteria were

collected by centrifugation for 15 min at $4,690 \times g$ and resuspended in 60 mL of lysis buffer

containing 0.2 M Tris, 1 mM EDTA, pH 8.0, supplemented with Halt EDTA-free protease

inhibitor cocktail (Thermo Scientific). The bacteria then were lysed on ice using a tip sonicator

set to 3 KJoule for 3×2 min cycles of 3 sec power on and 3 sec power off. The lysate was

centrifuged at $31,920 \times g$ for 20 min and the supernate was collected. The proteins were

precipitated from the supernatant by addition of 0.23g/ml ammonium sulfate. The solution with

the ammonium sulfate was stirred on ice for 20 min and centrifuged at $31,920 \times g$ for 20 min.

The supernatant was discarded and the protein pellets were dried. The pellets were resuspended

in 40 mL of 20 mM Tris, pH 8.0, and the resulting solution dialyzed overnight against 4 L of the

same buffer. The crude protein mixture was fractionated using ion-exchange Q columns (GE

Healthcare, Piscataway, NJ) and a 100 mL gradient ranging from 0 to 1.0 M NaCl in 20 mM

Tris, pH 8.0. The protein was purified further by size exclusion chromatography using a 2.15 ×

600 mm TSK-gel G3000SW column (Tosoh Biosciences, San Francisco, CA) with elution buffer comprising 100 mM sodium sulfate, 25 mM sodium phosphate, and 1 mM sodium azide, pH 6.5. Finally, the fractions containing purified ZF synuclein were dialyzed against 10 mM sodium phosphate, pH 7.4. The purity of the protein was assessed by SDS-PAGE and Coomassie blue staining.

Thioflavin T fluorescence assays

A concentrated protein solution was thawed on ice and filtered through a 0.2 μm filter prior to the fibril formation assay. Fibril formation assays were performed with 150-μM ZF γ1 or human α-syn as a positive control in 10 mM sodium phosphate, pH 7.4, and 10 μM thioflavin T (ThT). ThT is used for identification and staining of amyloid fibrils (Biancalana and Koide 2010). For inhibition assays with molecular tweezers, ZF γ1 was used at 100 μM. Stock solutions were made by dissolving CLR01 or CLR03 at 10 mM in 10 mM sodium phosphate, pH 7.4. CLR01 and CLR03 were added at the molar ratios indicated.

All assays were performed in black, Nunc 96-well optical bottom plates (Thermo Scientific). Teflon balls (1/8 inch in diameter) were distributed into each well of the 96-well plate. Then, 200 μL of solution (four replicates per sample) were pipetted into each well. The plate was agitated at 300 rpm with a 3-mm rotation diameter in a Varioskan microplate reader (Thermo Scientific) at 37 °C. Fluorescence measurements were recorded every 10-15 min by using $\lambda_{ex} = 444$ nm, $\lambda_{em} = 482$ nm, with an integration time of 200 μs.

The ThT fluorescence signal was corrected for the background by subtracting the mean fluorescence signal acquired during the first couple of hours since the start of the assay. The fluorescence signal was normalized by dividing each measurement by the mean signal collected

for 2–4 h during which the fluorescent reading had the largest value. If one of the sample

replicates had fluorescence reading close to the background, its fluorescence was normalized by

dividing it by the mean fluorescence reading of the remaining replicates. The data were

smoothed by substituting each data point with the average value calculated using six data points

collected before and after the point and the point itself. This is equivalent to central moving

average with a sliding thirteen-data-point-wide window. The normalized fluorescence signal of

ZF γ1 and CLR01 (ratio 1:1) and ZF γ1 and CLR01 (1:10), and ZF γ1 and CLR03 (1:10) were

calculated using the averaged fluorescence signal of maximum fluorescence acquired from the

assays of ZF γ1 alone.

Transmission Electron Microscopy (TEM)

Negatively stained specimens for TEM were prepared by applying 5 μL of sample onto

hydrophilic, 400-mesh, carbon-coated formvar support films mounted on copper grids (Ted

Pella, Inc.). The samples were allowed to adhere for 3 min, rinsed twice with distilled water and

stained for 1 min with 1% uranyl acetate. Grids were examined on JEM1200-EX (JEOL) or T12

(FEI) microscopes.

Statistical Analysis

Statistical analyses were performed using Student's t-test, log-rank, and one-way

ANOVA where appropriate. A minimum significance level was set at $p < 0.05$ for all studies.

Results

Ziram is toxic at low concentrations: ZF embryos exposed to ziram early in development

resulted in marked notochord malformations (see Fig. S2 b,c) similarly to other dithiocarbamates

(Haendel et al. 2004; Teraoka et al. 2006). In order to determine the toxicity of ziram without

this confound, embryos were exposed at 24 hpf, a developmental point at which the notochord is

sufficiently developed. When added at 24 hpf, ziram reduced survival in a concentration-

dependent manner. At 7 dpf, embryos appeared grossly normal but survival was reduced by 80%

at a concentration of 100 nM or above (see Fig. S2a).

Ziram is selectively toxic to DA neurons: We previously reported that ziram was

selectively toxic to DA neurons in rat primary mesencephalic cultures (Chou et al. 2008). In

order to determine if ziram is also toxic to DA neurons *in vivo*, we utilized a VMAT2:GFP ZF

line that expresses GFP driven by the VMAT2 promoter to monitor aminergic neuronal integrity

as previously described (Fitzmaurice et al. 2013; Wen et al. 2008). We tested ziram exposure at a

concentration of 50 nM since this was the highest concentration in which there was no

significant degree of lethality. A decrease in the number of GFP-labeled neurons was observed in

the telencephalic (TC) and diencephalic clusters (DC) (Figure 1a,b,c,d) in embryos treated with

ziram. These clusters are predominantly DA although they also include some noradrenergic

neurons (R. Jeroen Pasterkamp 2009; Rink and Wullimann 2002). The toxicity of ziram to DA

neurons was further supported by the measured 63% decrease in tyrosine hydroxylase-1 (TH-1)

protein levels (see Fig. S3). In order to determine if this toxicity was selective to aminergic

neurons, we measured the integrity of Rohon-Beard neurons after exposure to 50 nM ziram using

Tg(sensory:GFP) embryos as previously described (Fitzmaurice et al. 2013; Sagasti et al. 2005).

No significant change in the number of labeled sensory neurons was observed compared to

vehicle controls (Figure 1 e, f, and g). Furthermore, ziram appeared selectively toxic to DA

neurons since serotonergic neurons in the Raphe Nuclei of the VMAT2 transgenic line were

unaffected by ziram exposure (Figure 1 h,i,j).

Ziram alters ZF swimming behavior due to DA dysfunction: In light of the decrease in

DA neuron number, we asked if there was a behavioral phenotype of ziram toxicity that could be

attributed to DA neuronal loss. ZF embryos were treated with 50nM ziram at 24 hpf and

swimming was measured at 7 dpf in alternating light and dark cycles (Figure 2a). Vehicle-treated

ZF were much more active in the dark in a stereotypical manner as previously described

(Burgess and Granato 2007; Farrell et al. 2011). Ziram-treated fish swam significantly less in

the dark compared to controls but no change was seen in the light (Figure 2b,c). To determine if

these behavioral changes were due to DA neuronal dysfunction, we treated controls with the

dopamine antagonist haloperidol and found a similar pattern as with ziram, (i.e. less swimming

distance in the dark and no difference in the light). The decrease in swimming in ziram-treated

fish appeared to be secondary to a presynaptic dopamine loss since apomorphine, a potent

agonist of the dopamine receptors, stimulated swimming equally in ziram-treated and vehicle-

treated ZF (Figure 2b,c).

ZF γ1 *synuclein forms aggregates in vitro and in vivo:* α-syn aggregation appears to be

central to the pathophysiology of PD. Ziram increases α-syn levels in DA neurons in primary

mesencephalic cultures likely through inhibition of the proteasome (Chou et al. 2008; Wang et

al. 2006). Three isoforms of synuclein (β,γ1, and γ2) have previously been partially characterized

in ZF but none appear to be the exact orthologue to human α-syn (Milanese et al. 2012; Sun and

Gitler 2008). ZF γ1 has been previously demonstrated to be expressed widely throughout the

developing ZF brain (Chen et al. 2009). Since ZF γ1 synuclein contains N-terminal repeats and

hydrophobic regions similar to that of α-syn, and expression of human α-syn rescues behavioral

defects of γ1-deficient ZF embryos (Milanese et al. 2012), we investigated the propensity of ZF

γ1's to aggregate and induce toxicity *in vitro* and *in vivo*.

Recombinant human α-syn and ZF γ1 were incubated and monitored for β-sheet formation using ThT fluorescence. The morphology of each sample was examined at the end of the aggregation reactions by TEM (Sinha et al. 2012). The ThT fluorescence in the α-syn samples began to increase following a lag phase of ~10 h and reached a plateau at ~55 h (Figure 3A). In the ZF γ1 samples, the lag phase was shorter, ~7 h, and the kinetics of ThT fluorescence increase was faster, reaching a plateau by ~25 h (Figure 3A). Both proteins formed abundant fibrils as determined by TEM though the fibrils differed in length. α-Syn formed long fibrils, ≥1 μm in length with a diameter of 10 +/- 1nm (Figure 3B), whereas ZF γ1 formed 20-740nm long fibrils with a diameter of 9 +/- 2nm (Figure 3C). This difference in length and abundance of the fibrils can be attributed to ZF γ1's shorter nucleation rate, as reflected by the shorter ThT fluorescence lag phase relative to α-syn. Thus, similarly to α-syn and other amyloidogenic proteins, ZF γ1 is an amyloidogenic protein that has the ability to form β-sheet-rich fibrils.

We previously demonstrated that overexpression of α-syn in ZF neurons led to malformed embryos, intracellular aggregates, and neuronal death (Prabhudesai et al. 2012). Here, we overexpressed ZF γ1 in ZF neurons in order to determine if increased levels of endogenous protein induced aggregate formation, and were neurotoxic *in vivo*. In this model, ZF γ1 was expressed under control of the *HuC* neuronal promoter as a fusion protein with T2A-DsRed. The T2A peptide is post-translationally cleaved releasing native ZF γ1 and the fluorescent DsRed reporter in equal molar concentrations (Prabhudesai et al. 2012). Embryos overexpressing ZF γ1 were malformed and had reduced survival compared to embryos overexpressing DsRed (Figure 4a and b). Using an antibody specific for ZF γ1, we found that embryos overexpressing ZF γ1 formed intracytoplasmic aggregates (Figure 4c,d). Additionally, ThS staining was observed only in neurons overexpressing ZF γ1, whereas no staining was seen

in DsRed-expressing controls (Figure 4e and f) indicating that these aggregates contained β-sheet-rich aggregates.

Since ziram increases α-syn in primary neuronal cultures and ZF γ1 displays many of the same characteristics as α-syn, we determined the effects of ziram on ZF γ1 levels at 5 dpf. Western blot analysis of ZF embryo extracts probed with anti-ZF γ1 antibody revealed a band at 17 kDa (presumed monomer, Figure 5a and Fig. S1a). A significant decrease in intensity of the 17 kDa band was observed for embryos treated with 50nM ziram compared to vehicle-treated ZF (Figure 5b). Western blots conducted under native conditions revealed a major band of 480 kDa and a minor band at 242 kDa (see Fig. S1b) for both ziram-treated and control samples suggesting that ziram does not alter the degree of oligomerization of ZF γ1.

Ziram's toxicity is ZF γ1 dependent: In order to understand the role of ZF γ1 in ziram's neuronal toxicity, we knocked down ZF γ1 expression using MO prior to ziram treatment. MO knockdown of ZF γ1 protected telencephalic and diencephalic aminergic neurons from ziram's toxicity (Figure 6a,b).

To further explore the role of ZF γ1 in ziram's neuronal toxicity, we utilized the molecular tweezer, CLR01. CLR01 has previously been found to reduce human α-syn toxicity by disrupting α-syn aggregation *in vivo* and *in vitro* (Acharya et al. 2014; Prabhudesai et al. 2012; Sinha et al. 2012). We have previously reported that CLR01 reduced α-syn toxicity in cell-based models and in ZF (Prabhudesai et al. 2012). Here, we found that CLR01 also inhibited recombinant ZF γ1 fibrillation as determined by ThT fluorescence and EM (Figure 7 a-c) and reduced ziram's neurotoxicity *in vivo* as measured by the integrity of VMAT2:GFP neurons (Figure 7d). Thus, ziram's neurotoxicity appears to be dependent not only on the total ZF γ1

levels, as suggested by the MO experiment (Figure 6), but also on formation of toxic forms of ZF γ1, which are disrupted by CLR01 (Figure 7).

Discussion

The link between pesticide exposure and PD has become more recognized in recent years. The identification of specific toxins that increase PD risk such as paraquat, rotenone, ziram and maneb (Gatto et al. 2009; Tanner et al. 2009; Tanner et al. 2011; Wang et al. 2011), have facilitated mechanistic studies. Ziram has been shown to inhibit both the UPS and aldehyde dehydrogenase (ALDH) (Chou et al. 2008; Fitzmaurice et al. 2013; Fitzmaurice et al. 2014) but a direct link between these activities and neuronal toxicity *in vivo* is still lacking. In this study, we used a ZF model to study environmental toxins relevant to PD and found that ziram caused selective DA neuron damage with behavioral consequences. Since human α-syn is central to the pathogenesis of PD, we hypothesized that ZF γ1 mediates ziram's neurotoxicity. In support of this hypothesis, we found that ZF γ1 forms fibrils and is neurotoxic in a similar manner to human α-syn and that ziram's toxicity was ZF γ1-dependent.

Although ZF offer several advantages over other animal models when studying environmental toxins, there are a number of limitations that need to be considered. In all of our studies, we used developing embryos whereas PD is a disease of aging. Embryos were exposed at 24 hpf and formation of the blood-brain barrier begins at approximately 3 dpf (Fleming et al. 2013). Additionally, the metabolism of ziram might be different in ZF embryos compared to mammals since absorption at this early age may occur orally, dermally, or through the yolk. Despite these limitations, we believe our model is valid because the results are consistent with

previous studies performed in rodents where ziram and maneb have been shown to cause

selective DA-cell loss (Chou et al. 2008; Thiruchelvam et al. 2000).

The behavioral effect of ziram on ZF embryos appears to be caused by a specific

deficiency in DA signaling and not simply by non-specific toxicity. Ziram decreased locomotion

in the dark but not in the light in a similar manner as the dopamine antagonist haloperidol. This

decrease in activity was reversed by the dopamine agonist apomorphine suggesting that the

behavioral phenotype was due to a presynaptic dopamine deficiency. These results are

consistent with the apparent loss of VMAT2:GFP neurons. Less specific neurotoxins decrease

locomotion in both the light and the dark and would not be expected to be completely reversed

by a dopamine agonist. The selective loss of DA neurons by ziram is therefore supported by

both the behavioral data and the preservation of non-DA neurons (Rohon-Beard and serotonergic

neurons of the Raphe Nuclei). It is possible that the loss of GFP signal does not reflect neuron

loss but simply injury, yet the behavioral changes and the decrease in TH-1 support that ziram

caused DA neuron injury and dysfunction.

It is not completely clear how ziram causes selective DA neuron damage but the

mechanism appears to require ZF γ1. Others have previously demonstrated that ZF γ1 might

have a similar physiologic function as human α-syn (Milanese et al. 2012) in ZF, but we were

surprised to find that ZF γ1 is neurotoxic like α-syn. Here we demonstrate that recombinant ZF

γ1 formed amyloid fibrils with similar kinetics to α-syn, and overexpression of ZF γ1 in neurons

led to formation of aggregates and neurotoxicity in almost an identical manner to human α-syn

(Prabhudesai et al. 2012).

Previously, ziram was shown to inhibit the proteasome and increase accumulation of α-syn in primary neuronal cultures (Chou et al. 2008; Wang et al. 2006). Interestingly, we observed a decrease in protein levels of ZF γ1 in ziram-treated embryos. The differences in these results likely are due to the different models used, exposure times, and methods used to measure synuclein levels. In the neuronal culture study, ziram exposures were much shorter (48h) and synuclein levels were determined only in the soma of tyrosine hydroxylase-positive neurons. Since ziram decreases protein degradation by inhibiting the proteasome, we hypothesized that synuclein accumulated in the surviving neurons. In our current study, we measured total embryonic synuclein by Western blot analysis. Since synuclein is primarily a synaptic protein in differentiated neurons *in vivo*, we hypothesize that the lower levels we measured after 120h of treatment were due to neuronal terminal loss . DA terminal loss in these studies was confirmed by the reduction of GFP fluorescence in VMAT-2 neurons, reduction of TH immunoreactivity, and behavioral abnormalities that were reversed by a dopamine agonist. The fact that reducing ZF γ1 levels with MO almost completely protected against ziram toxicity suggests that ziram increased the formation of toxic ZF γ1 species early in embryonic development. Overexpression of ZF γ1 in neurons did lead to the formation of β-sheet-rich aggregates but we did not detect fibril formation with ThS *in vivo* after ziram exposure. The formation of synuclein β-sheets is dependent on several factors including concentration and time. In ziram treated embryos, ZF γ1 might not have reached high enough concentrations or had enough time to form aggregates. Regardless, others have suggested that prefibrillar oligomers of α-synuclein may be the cause of DA neuronal toxicity (Danzer et al. 2007; Winner et al. 2011). These data suggest that the toxic effect of ziram might be mediated by toxic, soluble ZF γ1 oligomers. This is supported by the finding that CLR01 also protected against ziram toxicity. CLR01 has previously been

demonstrated to act on amyloidogenic proteins and protect against their toxicity both *in vivo* and *in vitro* (Attar et al. 2012; Prabhudesai et al. 2012; Sinha et al. 2011). CLR01's only known activity is to remodel the self-assembly of amyloidogenic proteins into non-toxic and non-amyloidogenic structures and facilitate their clearance (Acharya et al. 2014; Attar and Bitan 2014; Prabhudesai et al. 2012).

Most neurodegenerative disorders like PD have a relatively selective pattern of neuronal loss although the mechanisms responsible for this selectivity have remained elusive. Ziram and other DTCs have been shown to inhibit the UPS, but this would not explain the selectivity of neuronal damage. It is possible that ziram's ability to inhibit ALDH in addition to its UPS-inhibiting activity, leads to selective DA damage. ALDH inhibition causes the accumulation of DOPAL in DA neurons, which is toxic (Burke et al. 2008; Casida et al. 2014; Fitzmaurice et al. 2013; Fitzmaurice et al. 2014; Panneton et al. 2010). The ZF model described here offers a powerful tool for further mechanistic studies.

Conclusions

In summary, we report that ziram, a pesticide that increases the risk of PD, causes selective DA neuron damage that is synuclein-dependent in ZF. These findings provide potentially important mechanistic implications on how ziram and possibly other environmental toxins can contribute to the pathogenesis of neurodegenerative disorders such as PD. A better understanding of these processes has the potential to illuminate pathways critical in disease formation and also highlight critical targets for future therapeutic exploitation.

References

Acharya S, Safaie BM, Wongkongkathep P, Ivanova MI, Attar A, Klarner FG, et al. 2014. Molecular basis for preventing alpha-synuclein aggregation by a molecular tweezer. The Journal of biological chemistry 289:10727-10737.

Agency USEP. 2015. Label amendment- remove use on blackberry on the label per epa request, product name: Ziram 76df fungicide. 70506-173. http://www3.epa.gov/pesticides/chem_search/ppls/070506-00173-20151002.pdf:Environmental Protection Agency.

Attar A, Ripoli C, Riccardi E, Maiti P, Li Puma DD, Liu T, et al. 2012. Protection of primary neurons and mouse brain from alzheimer's pathology by molecular tweezers. Brain : a journal of neurology 135:3735-3748.

Attar A, Bitan G. 2014. Disrupting self-assembly and toxicity of amyloidogenic protein oligomers by "molecular tweezers" - from the test tube to animal models. Current pharmaceutical design 20:2469-2483.

Baba M, Nakajo S, Tu PH, Tomita T, Nakaya K, Lee VM, et al. 1998. Aggregation of alpha-synuclein in lewy bodies of sporadic parkinson's disease and dementia with lewy bodies. The American journal of pathology 152:879-884.

Barnhill LM, Bronstein JM. 2014. Pesticides and parkinson's disease: Is it in your genes? Neurodegenerative disease management 4:197-200.

Betarbet R, Sherer TB, MacKenzie G, Garcia-Osuna M, Panov AV, Greenamyre JT. 2000.
Chronic systemic pesticide exposure reproduces features of parkinson's disease. Nature
neuroscience 3:1301-1306.

Biancalana M, Koide S. 2010. Molecular mechanism of thioflavin-t binding to amyloid fibrils.
Biochimica et biophysica acta 1804:1405-1412.

Bretaud S, Li Q, Lockwood BL, Kobayashi K, Lin E, Guo S. 2007. A choice behavior for
morphine reveals experience-dependent drug preference and underlying neural substrates in
developing larval zebrafish. Neuroscience 146:1109-1116.

Briquet M, Sabadie-Pialoux N, Goffeau A. 1976. Ziram, a sulfhydryl reagent and specific
inhibitor of yeast mitochondrial dehydrogenases. Archives of biochemistry and biophysics
174:684-694.

Brown TP, Rumsby PC, Capleton AC, Rushton L, Levy LS. 2006. Pesticides and parkinson's
disease--is there a link? Environmental health perspectives 114:156-164.

Burgess HA, Granato M. 2007. Modulation of locomotor activity in larval zebrafish during light
adaptation. The Journal of experimental biology 210:2526-2539.

Burke WJ, Kumar VB, Pandey N, Panneton WM, Gan Q, Franko MW, et al. 2008. Aggregation
of alpha-synuclein by dopal, the monoamine oxidase metabolite of dopamine. Acta
neuropathologica 115:193-203.

Casida JE, Ford B, Jinsmaa Y, Sullivan P, Cooney A, Goldstein DS. 2014. Benomyl, aldehyde
dehydrogenase, dopal, and the catecholaldehyde hypothesis for the pathogenesis of parkinson's
disease. Chemical research in toxicology.

Chartier-Harlin MC, Kachergus J, Roumier C, Mouroux V, Douay X, Lincoln S, et al. 2004. Alpha-synuclein locus duplication as a cause of familial parkinson's disease. Lancet 364:1167-1169.

Chen YC, Cheng CH, Chen GD, Hung CC, Yang CH, Hwang SP, et al. 2009. Recapitulation of zebrafish sncga expression pattern and labeling the habenular complex in transgenic zebrafish using green fluorescent protein reporter gene. Developmental dynamics : an official publication of the American Association of Anatomists 238:746-754.

Chou AP, Maidment N, Klintenberg R, Casida JE, Li S, Fitzmaurice AG, et al. 2008. Ziram causes dopaminergic cell damage by inhibiting e1 ligase of the proteasome. The Journal of biological chemistry 283:34696-34703.

Danzer KM, Haasen D, Karow AR, Moussaud S, Habeck M, Giese A, et al. 2007. Different species of alpha-synuclein oligomers induce calcium influx and seeding. The Journal of neuroscience : the official journal of the Society for Neuroscience 27:9220-9232.

Dorsey ER, Constantinescu R, Thompson JP, Biglan KM, Holloway RG, Kieburtz K, et al. 2007. Projected number of people with parkinson disease in the most populous nations, 2005 through 2030. Neurology 68:384-386.

Farrell TC, Cario CL, Milanese C, Vogt A, Jeong JH, Burton EA. 2011. Evaluation of spontaneous propulsive movement as a screening tool to detect rescue of parkinsonism phenotypes in zebrafish models. Neurobiology of disease 44:9-18.

Farrer M, Kachergus J, Forno L, Lincoln S, Wang DS, Hulihan M, et al. 2004. Comparison of kindreds with parkinsonism and alpha-synuclein genomic multiplications. Annals of neurology 55:174-179.

Feany MB, Bender WW. 2000. A drosophila model of parkinson's disease. Nature 404:394-398.

Fitzmaurice AG, Rhodes SL, Lulla A, Murphy NP, Lam HA, O'Donnell KC, et al. 2013. Aldehyde dehydrogenase inhibition as a pathogenic mechanism in parkinson disease. Proceedings of the National Academy of Sciences of the United States of America 110:636-641.

Fitzmaurice AG, Rhodes SL, Cockburn M, Ritz B, Bronstein JM. 2014. Aldehyde dehydrogenase variation enhances effect of pesticides associated with parkinson disease. Neurology 82:419-426.

Fleming A, Diekmann H, Goldsmith P. 2013. Functional characterisation of the maturation of the blood-brain barrier in larval zebrafish. PloS one 8:e77548.

Fokkens M, Schrader T, Klarner FG. 2005. A molecular tweezer for lysine and arginine. Journal of the American Chemical Society 127:14415-14421.

Gatto NM, Cockburn M, Bronstein J, Manthripragada AD, Ritz B. 2009. Well-water consumption and parkinson's disease in rural california. Environmental health perspectives 117:1912-1918.

Gatto NM, Rhodes SL, Manthripragada AD, Bronstein J, Cockburn M, Farrer M, et al. 2010. Alpha-synuclein gene may interact with environmental factors in increasing risk of parkinson's disease. Neuroepidemiology 35:191-195.

Goldman SM, Kamel F, Ross GW, Jewell SA, Bhudhikanok GS, Umbach D, et al. 2012. Head injury, alpha-synuclein rep1, and parkinson's disease. Annals of neurology 71:40-48.

Goldman SM. 2014. Environmental toxins and parkinson's disease. Annual review of pharmacology and toxicology 54:141-164.

Gunnarsson L, Jauhiainen A, Kristiansson E, Nerman O, Larsson DG. 2008. Evolutionary conservation of human drug targets in organisms used for environmental risk assessments. Environmental science & technology 42:5807-5813.

Haendel MA, Tilton F, Bailey GS, Tanguay RL. 2004. Developmental toxicity of the dithiocarbamate pesticide sodium metam in zebrafish. Toxicological sciences : an official journal of the Society of Toxicology 81:390-400.

Hope AD, Myhre R, Kachergus J, Lincoln S, Bisceglio G, Hulihan M, et al. 2004. Alpha-synuclein missense and multiplication mutations in autosomal dominant parkinson's disease. Neuroscience letters 367:97-100.

Ibanez P, Bonnet AM, Debarges B, Lohmann E, Tison F, Pollak P, et al. 2004. Causal relation between alpha-synuclein gene duplication and familial parkinson's disease. Lancet 364:1169-1171.

International Parkinson Disease Genomics C, Nalls MA, Plagnol V, Hernandez DG, Sharma M, Sheerin UM, et al. 2011. Imputation of sequence variants for identification of genetic risks for parkinson's disease: A meta-analysis of genome-wide association studies. Lancet 377:641-649.

Kruger R, Kuhn W, Muller T, Woitalla D, Graeber M, Kosel S, et al. 1998. Ala30pro mutation in the gene encoding alpha-synuclein in parkinson's disease. Nature genetics 18:106-108.

Maraganore DM, de Andrade M, Elbaz A, Farrer MJ, Ioannidis JP, Kruger R, et al. 2006. Collaborative analysis of alpha-synuclein gene promoter variability and parkinson disease. JAMA : the journal of the American Medical Association 296:661-670.

McCormack AL, Thiruchelvam M, Manning-Bog AB, Thiffault C, Langston JW, Cory-Slechta DA, et al. 2002. Environmental risk factors and parkinson's disease: Selective degeneration of nigral dopaminergic neurons caused by the herbicide paraquat. Neurobiology of disease 10:119-127.

Milanese C, Sager JJ, Bai Q, Farrell TC, Cannon JR, Greenamyre JT, et al. 2012. Hypokinesia and reduced dopamine levels in zebrafish lacking beta- and gamma1-synucleins. The Journal of biological chemistry 287:2971-2983.

Nishioka K, Hayashi S, Farrer MJ, Singleton AB, Yoshino H, Imai H, et al. 2006. Clinical heterogeneity of alpha-synuclein gene duplication in parkinson's disease. Annals of neurology 59:298-309.

Panneton WM, Kumar VB, Gan Q, Burke WJ, Galvin JE. 2010. The neurotoxicity of dopal: Behavioral and stereological evidence for its role in parkinson disease pathogenesis. PloS one 5:e15251.

Polymeropoulos MH, Lavedan C, Leroy E, Ide SE, Dehejia A, Dutra A, et al. 1997. Mutation in the alpha-synuclein gene identified in families with parkinson's disease. Science 276:2045-2047.

Prabhudesai S, Sinha S, Attar A, Kotagiri A, Fitzmaurice AG, Lakshmanan R, et al. 2012. A novel "molecular tweezer" inhibitor of alpha-synuclein neurotoxicity in vitro and in vivo.

Neurotherapeutics : the journal of the American Society for Experimental NeuroTherapeutics 9:464-476.

R. Jeroen Pasterkamp MPS, J. Peter H. Burbach. 2009. Development and engineering of dopamine neurons. Austin, Texas:Landes Bioscience.

Rink E, Wullimann MF. 2002. Development of the catecholaminergic system in the early zebrafish brain: An immunohistochemical study. Brain research Developmental brain research 137:89-100.

Ritz B, Rhodes SL, Bordelon Y, Bronstein J. 2012. Alpha-synuclein genetic variants predict faster motor symptom progression in idiopathic parkinson disease. PloS one 7:e36199.

Ryan SD, Dolatabadi N, Chan SF, Zhang X, Akhtar MW, Parker J, et al. 2013. Isogenic human ipsc parkinson's model shows nitrosative stress-induced dysfunction in mef2-pgc1alpha transcription. Cell 155:1351-1364.

Sagasti A, Guido MR, Raible DW, Schier AF. 2005. Repulsive interactions shape the morphologies and functional arrangement of zebrafish peripheral sensory arbors. Current biology : CB 15:804-814.

Schweitzer J, Lohr H, Filippi A, Driever W. 2012. Dopaminergic and noradrenergic circuit development in zebrafish. Developmental neurobiology 72:256-268.

Sheng D, Qu D, Kwok KH, Ng SS, Lim AY, Aw SS, et al. 2010. Deletion of the wd40 domain of lrrk2 in zebrafish causes parkinsonism-like loss of neurons and locomotive defect. PLoS genetics 6:e1000914.

Singleton AB, Farrer M, Johnson J, Singleton A, Hague S, Kachergus J, et al. 2003. Alpha-synuclein locus triplication causes parkinson's disease. Science 302:841.

Sinha S, Lopes DH, Du Z, Pang ES, Shanmugam A, Lomakin A, et al. 2011. Lysine-specific molecular tweezers are broad-spectrum inhibitors of assembly and toxicity of amyloid proteins. Journal of the American Chemical Society 133:16958-16969.

Sinha S, Du Z, Maiti P, Klarner FG, Schrader T, Wang C, et al. 2012. Comparison of three amyloid assembly inhibitors: The sugar scyllo-inositol, the polyphenol epigallocatechin gallate, and the molecular tweezer clr01. ACS chemical neuroscience 3:451-458.

Spillantini MG, Schmidt ML, Lee VM, Trojanowski JQ, Jakes R, Goedert M. 1997. Alpha-synuclein in lewy bodies. Nature 388:839-840.

Sun Z, Gitler AD. 2008. Discovery and characterization of three novel synuclein genes in zebrafish. Developmental dynamics : an official publication of the American Association of Anatomists 237:2490-2495.

Talbiersky P, Bastkowski F, Klarner FG, Schrader T. 2008. Molecular clip and tweezer introduce new mechanisms of enzyme inhibition. Journal of the American Chemical Society 130:9824-9828.

Tang W, Ehrlich I, Wolff SB, Michalski AM, Wolfl S, Hasan MT, et al. 2009. Faithful expression of multiple proteins via 2a-peptide self-processing: A versatile and reliable method for manipulating brain circuits. The Journal of neuroscience : the official journal of the Society for Neuroscience 29:8621-8629.

Tanner CM, Ross GW, Jewell SA, Hauser RA, Jankovic J, Factor SA, et al. 2009. Occupation and risk of parkinsonism: A multicenter case-control study. Archives of neurology 66:1106-1113.

Tanner CM, Kamel F, Ross GW, Hoppin JA, Goldman SM, Korell M, et al. 2011. Rotenone, paraquat, and parkinson's disease. Environmental health perspectives 119:866-872.

Teraoka H, Urakawa S, Nanba S, Nagai Y, Dong W, Imagawa T, et al. 2006. Muscular contractions in the zebrafish embryo are necessary to reveal thiuram-induced notochord distortions. Toxicology and applied pharmacology 212:24-34.

Thiruchelvam M, Richfield EK, Baggs RB, Tank AW, Cory-Slechta DA. 2000. The nigrostriatal dopaminergic system as a preferential target of repeated exposures to combined paraquat and maneb: Implications for parkinson's disease. The Journal of neuroscience : the official journal of the Society for Neuroscience 20:9207-9214.

Trinh J, Farrer M. 2013. Advances in the genetics of parkinson disease. Nature reviews Neurology 9:445-454.

Wang A, Costello S, Cockburn M, Zhang X, Bronstein J, Ritz B. 2011. Parkinson's disease risk from ambient exposure to pesticides. European journal of epidemiology 26:547-555.

Wang XF, Li S, Chou AP, Bronstein JM. 2006. Inhibitory effects of pesticides on proteasome activity: Implication in parkinson's disease. Neurobiology of disease 23:198-205.

Wen L, Wei W, Gu W, Huang P, Ren X, Zhang Z, et al. 2008. Visualization of monoaminergic neurons and neurotoxicity of mptp in live transgenic zebrafish. Developmental biology 314:84-92.

Winner B, Jappelli R, Maji SK, Desplats PA, Boyer L, Aigner S, et al. 2011. In vivo demonstration that alpha-synuclein oligomers are toxic. Proceedings of the National Academy of Sciences of the United States of America 108:4194-4199.

Xi Y, Noble S, Ekker M. 2011. Modeling neurodegeneration in zebrafish. Current neurology and neuroscience reports 11:274-282.

Figure Legends

Figure 1. Ziram is selectively toxic to dopaminergic neurons. VMAT2 ZF embryos were exposed to vehicle (a) and 50nM ziram (b) at 24 hpf. Neuronal counts for the telencephalic (TC) and diencephalic (DC) clusters were conducted at 5 dpf (n=5). A 30% decrease in telencephalic (c) and 39% decrease in diencephalic neurons (d), were observed in ziram-treated fish. Ziram's toxicity did not extend to Rohon-Beard neurons (5 dpf, n=7) after 50nM ziram exposure (f) compared to vehicle controls (e). Raphe Nuclei neurons are also labeled in VMAT2:GFP fish (serotonergic neurons) and were unaffected by ziram exposure (i) compared to vehicle controls (h). Raphe Nuclei neuron counts are shown in j. Scale bar = 500 μm. Two-tailed student t-test. *p<.05, **p<.01.

Figure 2. Ziram causes alterations in ZF motor behavior. Movement was tracked for larval ZF at 7 dpf (n=24). Distance's greater than 2 mm were tracked under an alternating light (yellow)/dark cycle (grey) (a). A 24.7% decrease (p<.05) in distance traveled during periods of dark was observed in ziram-treated ZF relative to vehicle-treated ZF(b) but no significant difference was observed in the light (c). A similar pattern of swimming, less in the dark but no difference in the light, was measured when ZF were treated with the dopamine antagonist haloperidol (b and c). The dopamine agonist apomorphine increased swimming to a similar degree in the ziram-treated and control ZF suggesting that the post-synaptic dopaminergic system remains intact. No significant difference in motor behavior was observed for ziram + apomorphine vs. apomorphine alone for light or dark conditions. All treatment groups were

compared to vehicle control for statistical analysis. *p<.05, ***p<.001, ****p<.0001, one way

ANOVA.

Figure 3. ZF γ1 synuclein aggregates and forms fibrils similarly to human α-synuclein.

Recombinant human α-syn (hSyn) or ZF γ1 (both 150μM) were incubated over a 66-hour period

and thioflavin T fluorescence was monitored (a). The morphology of hSyn (B) and ZF γ1 (c) was

examined at the end of the aggregation reaction using TEM (scale bar = 0.2 μm).

Figure 4. Overexpression of ZF γ1 *in vivo* causes intracellular aggregation of synuclein.

Embryos were injected with constructs for Huc-T2A-DsRed (a) or Huc-γ1-T2A-DsRed (b),

embryos shown at 2 dpf (scale bar = 100 μm). Sectioned embryos were stained with a primary

antibody for ZF γ1. HuC-DsRed (c) injected embryos did not have intracellular ZF γ1

aggregates, while embryos injected with HuC-ZFγ1 (d) were found to have intracellular ZF γ1

aggregates (blue arrow) (scale bar = 10 μm). To determine if ZF γ1 formed β-pleated sheets *in

vivo*, embryos injected with HuC-DsRed and Huc-γ1-T2A-DsRed were stained with ThS (scale

bar = 10 μm). Only neurons overexpressing ZF γ1 (f) were ThS positive (e).

Figure 5. Ziram decreases ZF γ1 levels. Embryos were treated with ziram or vehicle and ZF γ1

levels were determined by Western blot analysis at 5dpf (normalized to tubulin). A 69.3%

decrease in band density for ZF γ1 was observed for samples treated with 50nM ziram (a,b, n=4).

*p<.05 two-tailed student t-test.

Figure 6: Ziram's toxicity is ZF γ1-dependent. ZF γ1 expression was reduced using a specific

morpholino (MO) and a scrambled MO was used as a control. Ziram treatment began at 24 hpf.

Neuronal counts (normalized to vehicle + scramble/γ1 MO) for γ1 MO injected embryos (n=14).

An 86.8% increase in labeled telencephalic (a) and 45.1% increase in labeled diencepahlic (b)

VMAT2 neurons at 3dpf was observed for fish treated with ziram + γ1 MO vs. ziram + scramble

MO. *p<.05, **p<.01, student t-test

Figure 7. CLR01 inhibits ZF γ1 aggregation in vitro and protects against ziram's toxicity in

vivo. Time-dependent change in normalized ThT fluorescence over 14 days for 100 μM γ1

incubated in the absence or presence of CLR01 (a). The first and last 130 hours are shown

(N=4). Electron micrographs of ZF γ1 alone (b), and ZF γ1 with CLR01 (c) in equimolar ratio

(scale bar = 100 nm) obtained on day 9 or 10 of each reaction (ANOVA, p < 0.0001). CLR01

treatment protected against ziram toxicity (50nM; n=6) to VMAT2 neurons in the diencephalic

cluster (e) but did not reach statistical significance in the telencephalic cluster (d) at 5 dpf.
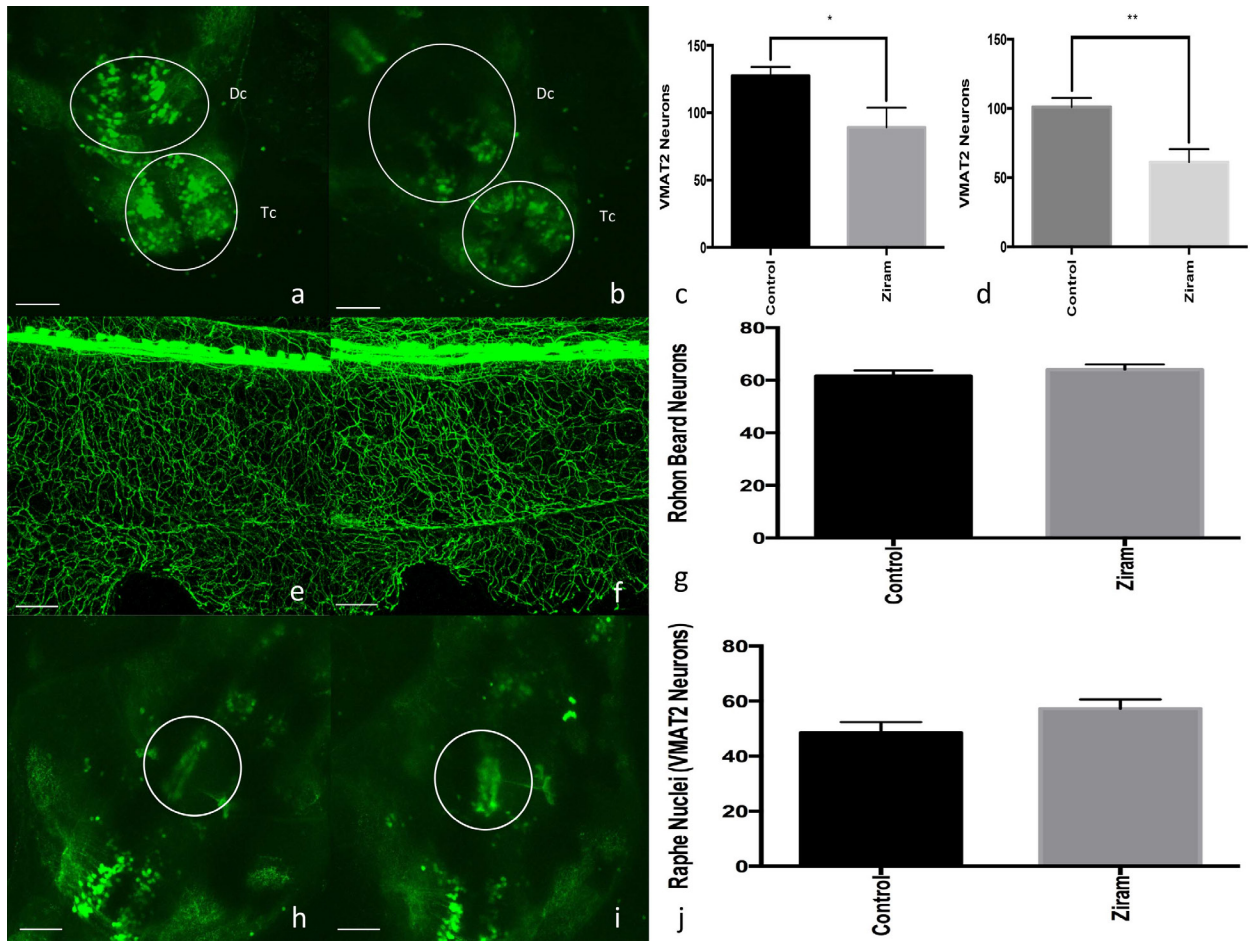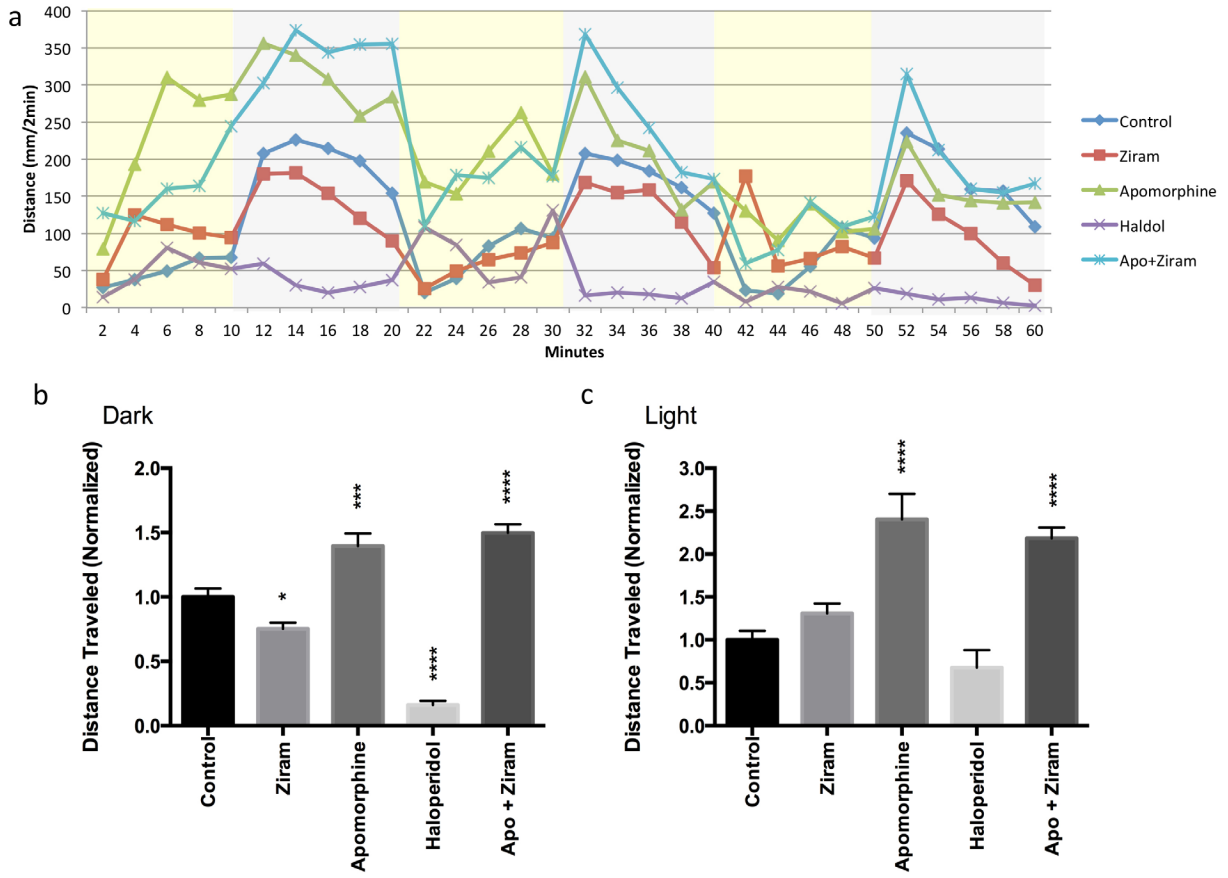
**p<.01, student t-test.
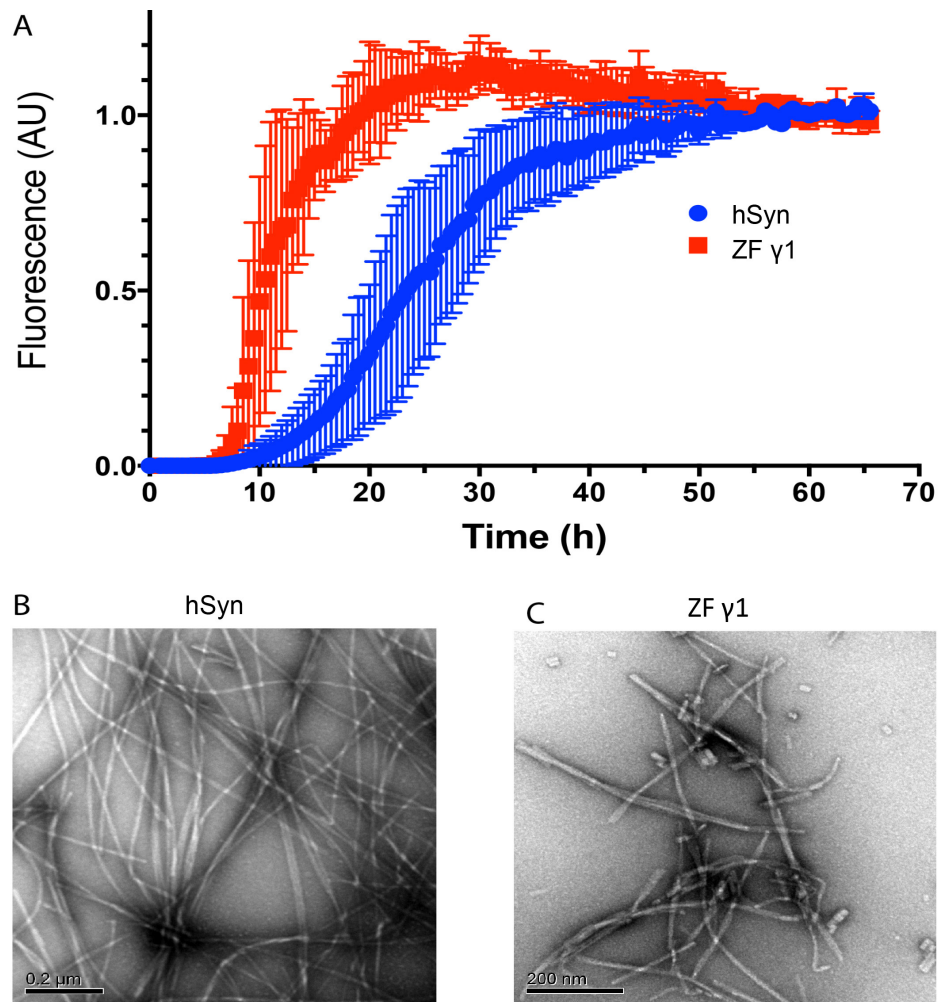
Figure 1.

Figure 2.

Figure 3.

Figure 4.

Figure 5.

a

γ1   Control   Ziram

17 —

Tubulin   Control   Ziram

b

Figure 6.

a

b

Figure 7.